Journal Pre-proof

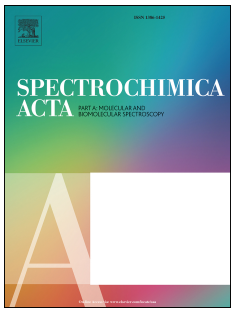

Fluorescent schiff base probes for sequential detection of Al^{3+} and F^{-} and cell imaging applications

Jiaxin Fu, Bai Li, Huihui Mei, Yongxin Chang, Kuoxi Xu

PII: S1386-1425(19)31068-6

DOI: https://doi.org/10.1016/j.saa.2019.117678

Reference: SAA 117678

To appear in: *Spectrochimica Acta Part A: Molecular and Biomolecular Spectroscopy*

Received Date: 13 September 2019

Revised Date: 28 September 2019

Accepted Date: 17 October 2019

Please cite this article as: J. Fu, B. Li, H. Mei, Y. Chang, K. Xu, Fluorescent schiff base probes for sequential detection of Al^{3+} and F^{-} and cell imaging applications, *Spectrochimica Acta Part A: Molecular and Biomolecular Spectroscopy* (2019), doi: https://doi.org/10.1016/j.saa.2019.117678.

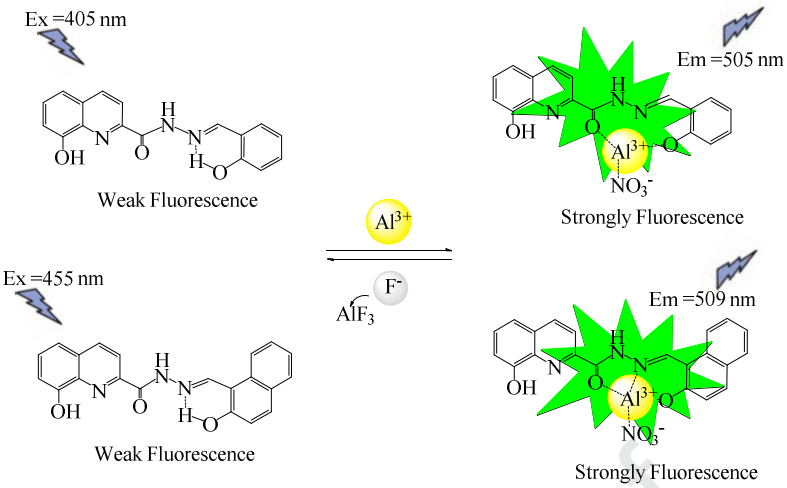

8-Hydroxyquinoline-based probes **SQ** and **NQ** revealed excellent selective recognition towards Al^{3+} with obvious vision changes of color in DMSO-H_2O (1/2, v/v) solution. The both complexes **SQ**-Al^{3+} and **NQ**-Al^{3+} can further detect F^- with the detection limits 1.64×10^{-7} and 3.58×10^{-8} M, respectively. The fluorescence spectra, UV spectra, HRMS and so on were used to obtain a 1:1 complex between the sensors **SQ** and **NQ** and Al^{3+}, and the complexation mode between the complexes was inferred by nuclear magnetic titration. In addition, filter paper and cell imaging experiments proved the probes **SQ** and **NQ** had the potential application value to monitor Al^{3+} and F^- in environment and vivo.

Fluorescent schiff base probes for sequential detection of Al^{3+} and F^{-} and cell imaging applications

Jiaxin Fu, Bai Li, Huihui Mei, Yongxin Chang, Kuoxi Xu*

College of Chemistry and Chemical Engineering, Henan University, Kaifeng 475004, Henan, China

Abstract: Two novel Schiff-base fluorescent probers **SQ** and **NQ** based on 8-hydroxyquinoline moiety were designed and synthesized. The both probes were capable of binding with Al^{3+} by naked eye detection to produce a significant fluorescence enhancement response with a detection limit of 1.48×10^{-8} and 4.23×10^{-8} M, respectively. At the same time, the formed complexes **SQ**-Al^{3+} and **NQ**-Al^{3+} could sequentially detect F^{-}, and the detection limits of F^{-} were determined to be 1.64×10^{-7} and 3.58×10^{-8} M, respectively. The "off-on-off" fluorescence response process demonstrated that the binding were reversible. The probes were further successfully utilized to detect Al^{3+} and F^{-} in vitro PC12 cells.

Keywords: Schiff base; Visible sensing; Al^{3+} and F^{-}; off-on-off; Cells imaging

1. Introduction

Among variant analytes, the role of metal ions in environment and living organisms cannot be ignored, particularly Al^{3+}, distributing in all corners of the earth and frequently utilized in various fields, such as high tension wire, space shuttle, kitchenware and clinical drugs [1]. Nevertheless, soil acidity increasing Al^{3+} ion caused is detrimental to growing crops [2, 3] and marine lives. The toxic impact of Al^{3+} ion is not only known to affect the plants and aquatic ecosystem but also confined to humans. It is threatening even deadly that exposure of mankind to the inevitable aluminium environment for a long time, which probably poses several neurodegenerative diseases, including representative Alzheimer's disease [4] and Parkinson's disease [5], as well as glucose intolerance, memory loss and cardiac arrest [6, 7]. Though conventional analytical techniques like as atomic absorption spectrometry (AAS) [8, 9], ion chromatography (IC) [10, 11] and inductively coupled plasma mass spectrometry (ICP-MS) [12, 13] are employed to detect ions or neutral molecule at short intervals. However, the vital drawbacks still exist where cumbersome pretreatment test only in vitro, poor real-time monitoring and high maintenance costs make them subject to a good deal of restrictions in practical applications. Fluorescent probe, as the crucial research realm of supramolecular

* Corresponding author. E-mail addresses: xukx@henu.edu.cn.

chemistry, occupies a valuable position in molecular recognition, which is relevant to its traits containing facile operational procedures, high selectivity and sensitivity in fluorescent assays [14-16], alongside the possibility of applications in biologically and environmentally pertinent species [17-19]. Although many Al^{3+} fluorescent probes have been developed, there still exist some shortages, such as suffering from the interferences of Fe^{3+}, Cu^{2+} and Zn^{2+} ions, poor water-solubility. Thus it is indispensable and pressing to go in quest of highly selective and sensitive Al^{3+} fluorescent probe. Meanwhile, the function of anions cannot be neglected as well on the environment and biology, particularly F^-, which plays the part of the field of biology and environment, such as pharmaceutical agent, therapy of osteoporosis and prevention of dental caries [20, 21]. The disorder of F^- is in charge of several diseases containing stomach ulcer and urolithiasis [22, 23], and hence it is high time to identify F^- to guard against related untoward conditions.

8-Hydroxyquinoline and its derivatives were selected for synthesis not only as fluorophore and recognition group, but also due to the features of high absorption coefficient, long-wave absorption and emission wavelength after modification. Considering that poor coordination ability of Al^{3+} compared to transition metals and the lack of spectroscopic chatacteristics [24, 25], the introduction of the C=N double bond also enhances its ability of selection and recognition for Al^{3+}. So Schiff-base ligands 8-hydroxy-N'-(2-hydroxybenzylidene)quinoline-2-carbohydrazide **SQ** and 8-hydroxy-N'-((2-hydroxynaphthalen-1-yl)methylene)quinoline-2-carbohydrazide **NQ** based on 8-hydroxyquinoline were applied in this paper to detect Al^{3+} and F^- [26, 27]. The detection of F^- through particular interactions between Al^{3+} and F^- utilize the non-covalent interactions with low energy to form $[AlF_x]^{n-}$ complex [28, 29], which saves the cost, enhances specific recognition and flexibility. Due to excited-state intramolecular proton transfer (ESIPT) and C=N isomerization, the fluorescence intensities of **SQ** and **NQ** were greatly reduced, but once combining with Al^{3+} to form complexes, the rigid chelation structure of the whole systems were turned up and the fluorescence intensity were greatly improved. While the fluorescence of the resulting

complex quenched by interacting with F^- and the "off-on-off" fluorescent changes were reflected by changes in the spectrum (UV-vis and fluorescence). These analytical phenomena were also supported in PC12 cell imaging experiments and indicated the potential of applications in *vivo*.

Compared with some of the fluorescent probes recently released for Al^{3+} ion detection [30-36], in general, our probes have some advantages over other probes, while the other probes rarely do better. First, association constant (Ka) represents for the tightness between host and guest. The Ka values of **SQ** and **NQ** are greater than that of most. Besides, detection limit means the sensitivity of probes towards analyte. Our probes illustrate 10^{-8} M sensitivity to metal ions, while few probes evince values in this range. Finally, our probes both accomplish the anion recognition, paper test and cell image. Comprehensive comparison is listed in the Table 1.

Table 1 Performance comparison of recently published probes

Entry	Probe	Media	Target	Ka (M^{-1})	Detection limit (M)	Application	Reference
1	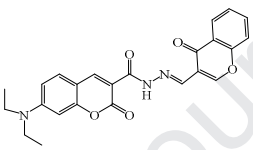	EtOH	Al^{3+}	1.32×10^4	1.44×10^{-7}	photographs of coated test papers	[30]
2	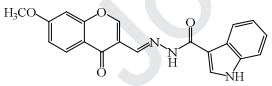	EtOH	Al^{3+}	2.50×10^3	1×10^{-7}	/	[31]
3	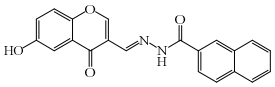	EtOH/ H_2O	Al^{3+}	1.30×10^4	3.48×10^{-8}	photograph of coated test paper	[32]
4	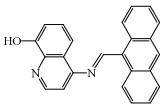	MeCN/ H_2O	Al^{3+}	2.10×10^2	1.08×10^{-6}	Cell imaging	[33]
5	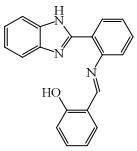	MeOH/ PBS	Al^{3+}	2.61×10^5	3.1×10^{-7}	Cell imaging	[34]
6	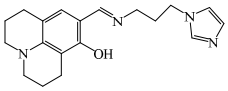	MeCN/ H_2O	Al^{3+}	2.0×10^7	3.9×10^{-6}	Anion recognition	[35]

7	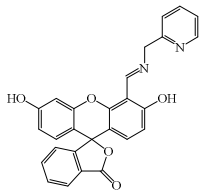	Tris-HCl buffer	Al^{3+}	/	9.2×10^{-8}	Anion recognition; Cell imaging	[36]
8	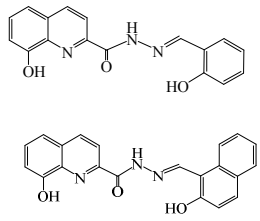	DMSO/ H_2O	Al^{3+}	9.40×10^{4} 9.40×10^{4}	1.48×10^{-8} 4.23×10^{-8}	Anion recognition; paper test; Cell imaging	This work

2. Materials and methods

2.1. Materials and instrumentation

IR spectra was measured using a Nicolet 670 FT-IR spectrophotometer. ^{1}H NMR and ^{13}C NMR was recorded on Bruker-AV-400 NMR spectrometer. UV-visible absorption spectra was acquired on a Perkin-Elmer Lamda-25 UV-Vis spectrophotometer. Electrospray ionization mass spectrometry (ESI-MS) spectra was measured on a Brukerama Zon SL mass instrument. Fluorescence spectral was carried out in an F-7000 fluorescence spectrophotometer. The melting point was taken on a MEL-TEMP II melting point apparatus. The fluorescence quantum yield was evaluated with JY HORIBA FluoroLog-3 Steady-Transient fluorescence spectrometer. The reagents and pharmaceuticals referred herein were available from commercial suppliers and used without further processed. The metal ions used were all nitrate or chloride salts, and the anions were tetrabutylammonium or sodium. The intermediate compound **1** was prepared with the reported literatures [37, 38].

2.2. Analysis

The nitrate or chloride salt of various metal ions and the tetrabutylammonium or sodium salt of anions were separately dissolved in 3 mL deionized water to prepare a stock solution for concentration of 0.1 M, and the corresponding volume was taken up using a micro syringe during spectrometry. **SQ** or **NQ** were formulated into a DMSO stock solution of 0.01 M, and diluted to 3.33×10^{-5} M in a cuvette containing

DMSO-H_2O (1/2, v/v) solution for analysis. The test solution volume was 3 mL. In the fluorescence spectroscopy experiment, different concentrations of metal ions were added separately to a series of **SQ** or **NQ** solutions and mixed evenly; next the fluorescence intensity of every system after addition were recorded to judge the identified metal ion. The screening process of anion was similar to the method above. Then the affinity of **SQ** or **NQ** was evaluated to recognize Al^{3+} or F^- in the presence of other interfering ions. During the titration experiment, Al^{3+} or F^- was gradually added to the single **SQ** or **NQ** system until equilibrium, and the UV-vis or fluorescence spectrum data were collected uniformly. The excitation wavelengths of **SQ** and **NQ** were 405 and 455 nm, respectively. In the ^1H NMR titration experiment, Al^{3+} with different concentrations were added to several DMSO-d_6 solutions containing **SQ** or **NQ**, and the chemical shifts were observed.

2.3. Synthesis:

Compound **1**: ^1H NMR ($CDCl_3$) δ 10.22 (s, 1H), 8.32 (d, *J* = 8.5 Hz, 1H), 8.16 (s, 1H), 8.06 (d, *J* = 8.5 Hz, 1H), 7.63 (t, *J* = 8.0 Hz, 1H), 7.43 (d, *J* = 7.8 Hz, 1H), 7.29 (d, *J* = 7.7 Hz, 1H).

Compound **2**: Compound **1** (0.43 g, 2.50 mmol) was placed in a round bottom flask, 20 mL of 30 % H_2O_2 and 2 drops of formic acid were added, and the reaction was stirred at room temperature for 8 h until a yellow precipitate appeared. The solid was filtered and dried to give compound **2**. Yield: 96 %. ^1H NMR (DMSO-d_6) δ 10.23 (s, 1H), 8.57 (d, *J* = 8.5 Hz, 1H), 8.15 (d, *J* = 8.5 Hz, 1H), 7.64 (t, *J* = 7.9 Hz, 1H), 7.54 (d, *J* = 8.2 Hz, 1H), 7.22 (d, *J* = 7.6 Hz, 1H).

Compound **3**: Thionyl chloride (0.5 mL) was added dropwise into a continuously stirring round bottom flask containing 15 mL of methanol in an ice bath, then compound **2** (0.47 g, 2.50 mmol) was added to the above system and the reaction was refluxed for 6 h under N_2 protection. After the reaction, the solvent was evaporated under reduced pressure to give compound **3** as orange solid. Yield: 82%. ^1H NMR ($CDCl_3$) δ 8.24 (d, *J* = 8.5 Hz, 1H), 8.11 (d, *J* = 8.5 Hz, 1H), 7.51 (t, *J* = 8.0 Hz, 1H),

7.33 (d, *J* = 8.2 Hz, 1H), 7.18 (d, *J* = 5.6 Hz, 4H), 5.23 (s, 1H), 4.00 (s, 2H).

Compound **4**: Compound **3** (0.50 g, 2.50 mmol) was dissolved in a round bottom flask with 15 mL of ethanol, then 80 % hydrazine hydrate (0.93 mL, 15.00 mmol) was added and refluxed for 8 h. After the reaction cooled, the solid was precipitated, filtered, washed with ethanol and dried to give compound **4** as yellow solid. Yield: 87%. ^{1}H NMR (DMSO-d_6) δ 10.78 (s, 1H), 8.49 (d, *J* = 8.5 Hz, 1H), 8.12 (d, *J* = 8.5 Hz, 1H), 7.55 (t, *J* = 7.9 Hz, 1H), 7.47 (d, *J* = 8.1 Hz, 1H), 7.15 (d, *J* = 7.5 Hz, 1H), 4.66 (s, 2H).

SQ and **NQ:** Salicylaldehyde (0.31 mL, 3.00 mmol) or 2-hydroxy-1-naphthaldehyde (0.50 g, 3.00 mmol) was added to a round bottom flask containing compound **4** (0.51 g, 2.50 mmol) in methanol (20 mL), and refluxed for 6 h, finally the precipitate was filtered and dried.

SQ: yield: 86 %. Mp: 129.6-130.7 □. ^{1}H NMR (DMSO-d_6) δ 12.66 (s, 1H), 11.08 (s, 1H), 10.19 (s, 1H), 8.87 (s, 1H), 8.59 (d, *J* = 8.6 Hz, 1H), 8.25 (d, *J* = 8.5 Hz, 1H), 7.68 (d, *J* = 7.7 Hz, 1H), 7.63 (t, *J* = 7.9 Hz, 1H), 7.54 (d, *J* = 8.1 Hz, 1H), 7.35 (t, *J* = 7.2 Hz, 1H), 7.24 (d, *J* = 7.5 Hz, 1H), 6.99 (d, *J* = 3.9 Hz, 1H), 6.97 (t, *J* = 8.1 Hz, 1H); ^{13}C NMR (DMSO-d_6) δ 160.30, 157.87, 154.10, 149.02, 146.91, 138.62, 136.85, 132.16, 130.38, 130.25, 129.37, 119.98, 119.62, 119.46, 118.22, 116.93, 112.37; IR (KBr) cm^{-1}: 3452, 3203, 1622, 1500, 1366, 1158, 747; MS: Calcd for: [M+H]$^{+}$: 308.1030, Found: 308.1033.

NQ: yield: 89 %. Mp: 264.2-264.7 □. ^{1}H NMR (DMSO-d_6) δ 12.83 (s, 1H), 12.61 (s, 1H), 10.19 (s, 1H), 9.58 (s, 1H), 8.61 (d, *J* = 8.5 Hz, 1H), 8.53 (d, *J* = 8.6 Hz, 1H), 8.27 (d, *J* = 8.5 Hz, 1H), 7.98 (d, *J* = 9.0 Hz, 1H), 7.92 (d, *J* = 8.0 Hz, 1H), 7.64 (t, *J* = 7.8 Hz, 2H), 7.56 (d, *J* = 8.1 Hz, 1H), 7.44 (t, *J* = 7.4 Hz, 1H), 7.29 (d, *J* = 5.4 Hz, 1H), 7.27 (d, *J* = 4.0 Hz, 1H); ^{13}C NMR (DMSO-d_6) δ 160.23, 158.65, 154.10, 148.17, 146.83, 138.66, 136.90, 133.52, 132.09, 130.42, 130.29, 129.44, 128.40, 128.32, 124.10, 121.89, 119.65, 119.31, 118.28, 112.42, 109.33; IR (KBr) cm^{-1}: 3373, 3226, 1655, 1502, 1464, 1391, 1324, 1239, 1192, 956; MS: Calcd for: [M+H^{+}]: 358.1186, Found: 358.1190.

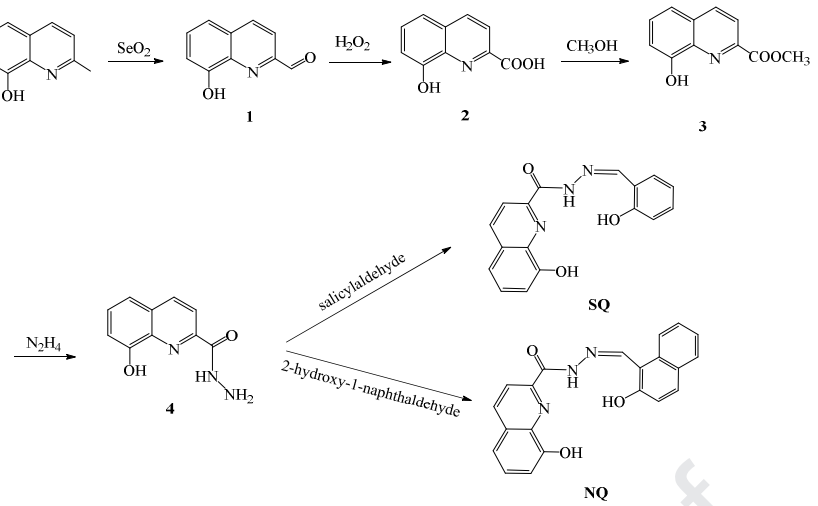

Scheme 1 Synthetic route of **SQ** and **NQ**.

2.4. MTT assay and Cell imaging studies

PC12 cells were cultivated with fetal bovine serum (10 %) in Dulbecco's modified Eagle's medium (DMEM) at 37 °C and 5% CO_2 for 24 h. To begin with, MTT assay was carried to assess the toxicity of **SQ** and **NQ** in PC12 cells at different concentrations 0, 30, 60, 90, 120 μM and then monitor the livability. Probe with applicable concentration 10 μL was selected to incubate with PC12 cells at 37 °C for 0.5 h in PBS buffered solution, which were washed with PBS (phosphate-buffered saline) buffered solution to eradicate the disturbance of residue probe in the extracellular media. In addition, the cells with probe were incubated with Al^{3+} another for 0.5 h. Then F^- was added in the same ways. The cells were observed under the DMI8 inverted fluorescence microscope after every treatment.

3. Results and discussion

3.1. Synthesis and characterization

Taking 8-hydroxyquinaldine as a raw material, the quinoline carboxylic acid compound **2** was obtained by two oxidations via SeO_2 and H_2O_2, and then compound **4** was obtained by esterification reaction with methanol and subsequent trapping, which finally condensed with salicylaldehyde or 2-hydroxy-1-naphthaldehyde to give final compounds **SQ** and **NQ**, respectively (Scheme 1). The structures were

confirmed by IR, ^{1}H NMR, ^{13}C NMR and HRMS (Fig. s1-s7).

*3.2. Spectroscopic studies of probe **SQ** and **NQ** on Al^{3+}*

Initially, the fluorescence selectivity experiments of **SQ** and **NQ** were carried out on metal ions. Almost no fluorescence emission peaks of **SQ** (λ_{ex}: 405 nm, Φ = 0.51) and **NQ** (λ_{ex}: 455 nm, Φ = 2.39) were observed in the DMSO-H_2O solution (1/2, v/v). When Li^+, Na^+, K^+, Ag^+, Mg^{2+}, Ca^{2+}, Al^{3+}, Co^{2+}, Ni^{2+}, Cu^{2+}, Fe^{2+}, Mn^{2+}, Pb^{2+}, Zn^{2+}, Ba^{2+}, Hg^{2+}, Cd^{2+}, Cr^{3+}, Fe^{3+} ions were added respectively into several solutions including **SQ** or **NQ**, it was found that no obvious fluorescence changes except for Al^{3+} (Fig. 1). Once Al^{3+} existed, **SQ** and **NQ** had prominent 270-fold (Φ = 0.86) and 460-fold (Φ = 7.16) fluorescence enhancement at 505 nm and 509 nm, separately, alongside the colors of both systems changed from colorless to green (under UV-light 365 nm).

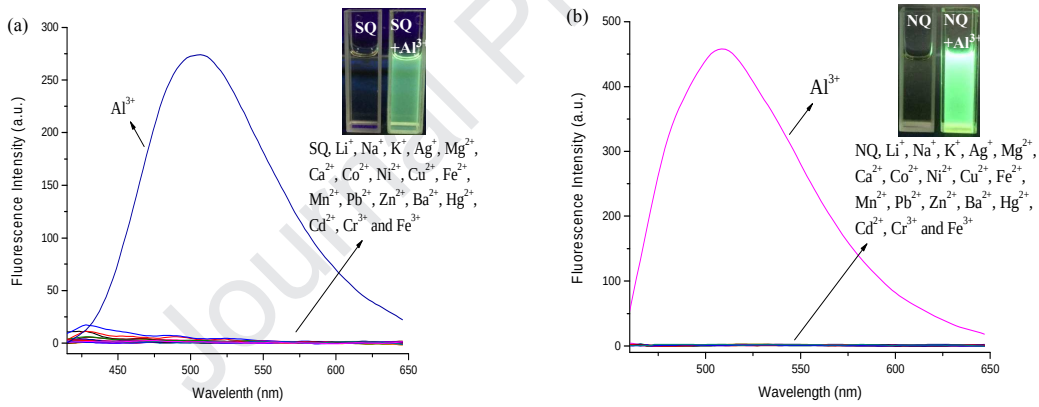

Fig. 1. Fluorescence spectrum changes of the **SQ** (a) or **NQ** (b) solution (3.33×10^{-5} M) after separately different metal ions added in DMSO-H_2O (1/2, v/v) solution, inset: color change of **SQ** solution before and after adding Al^{3+} ion. Inset: color change of the **NQ** or **NQ** solution before and after the addition of Al^{3+}.

On top of the phenomenon above, the competition experiment further verified the specific selectivity of **SQ** and **NQ** for Al^{3+}. With different interfering ions (5 equiv.) aforementioned added into the **SQ** and **NQ** solution, the fluorescence intensities had no significant effect. Then Al^{3+} was added continuously, and the fluorescence emission data were collected and the intensity values were compared before and after the addition of Al^{3+}, and drastically enhancement appeared, which illustrated that **SQ** and **NQ** were more intimate to Al^{3+} in the presence of other

interfering ions and had excellent fluorescence selectivity for Al^{3+} ion (Fig. s8).

In order to investigate the recognition performance of **SQ** and **NQ** for Al^{3+}, a fluorescence titration experiment was performed. During the titration, fluorescence intensity of **SQ** or **NQ** augmented with the incremental concentration for Al^{3+}. When the Al^{3+} concentration reached 2.52 and 5.00 equiv., respectively, the fluorescence intensity of **SQ** or **NQ** became steady at 505 nm and 509 nm (Fig. 2). This phenomenon can be explained by the fact that the imine structure usually makes the fluorescence of the system weak, partly due to the intramolecular -C=N- double bond isomerization in the excited state [39, 40], and partly due to the ESIPT [41], in which protons are transferred from phenol to methylimine N atom. But after forming a stable complex with Al^{3+}, both processes are inhibited, the molecular rigid structures are formed, and the chelation between the host and the guest also made fluorescence enhancement (CHEF), so that the apparent fluorescence-enhanced responses are captured [42, 43]. According to the fluorescence titration data, a linear fit with the Benesi-Hildebrand equation [44, 45] to obtain the complex constants (Ka) of **SQ** and **NQ** with Al^{3+} were both 9.40×10^{4} M^{-1} (Fig. 3), and the detection limits towards Al^{3+} were 1.48×10^{-8} and 4.23×10^{-8} M (Fig. s9) (3σ/S, where σ is deviation of the blank signal and S is slope of calibration curve), which met the limit about drinking water according to the WHO standard (7.41 μM) [46, 47].

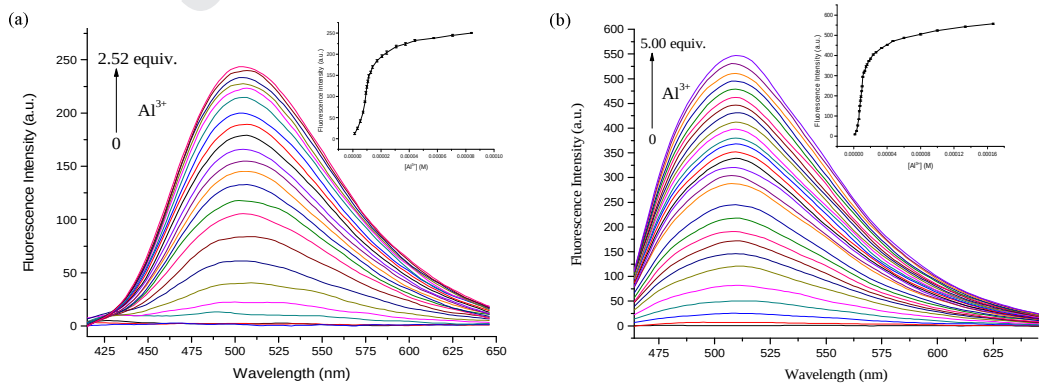

Fig. 2. (a) Fluorescence spectral changes of the **SQ** (3.33×10^{-5} M) solution with different ratios of Al^{3+} (0-2.52 equiv.) added in the DMSO-H_2O (1/2, v/v); (b) Fluorescence spectral changes of the **NQ** (3.33×10^{-5} M) solution with different ratios of Al^{3+} (0-5.00 equiv.) added in the DMSO-H_2O (1/2, v/v). Insert: error bars were obtained from the standard deviation of three replicate experiments.

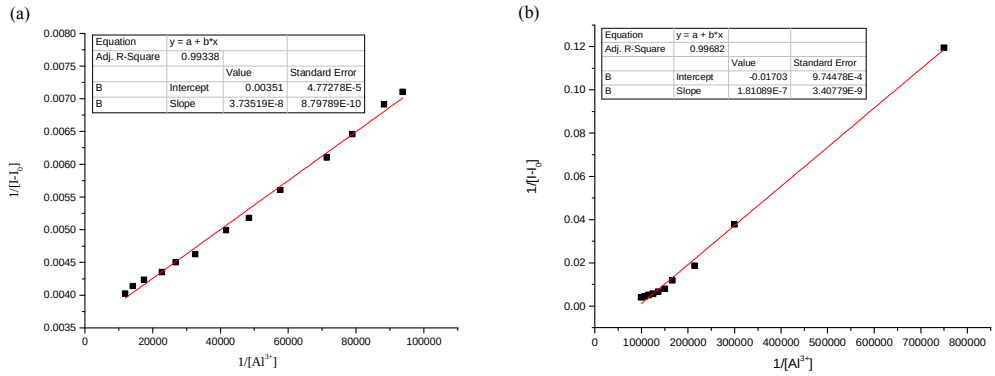

Fig. 3. (a) Linear fitting with the Benesi-Hildebrand equation of **SQ** and Al^{3+} for complexing constant Ka_1= 9.40×10^4 M^{-1} (R^2 = 0.9934); (b) Linear fitting of **NQ** and Al^{3+} with Benesi-Hildebrand equation for the complexation constant Ka_2= 9.40×10^4 M^{-1} (R^2 = 0.9968).

In the UV spectroscopy experiment, as shown in Fig. 4, free **SQ** had three main UV absorption peaks, and the UV absorption peaks at 257 nm and 296 nm were mainly due to intramolecular n-π* electronic transitions and imines -C=N- structure, while UV absorption at 340 nm was attributed to intramolecular π-π* electronic transitions and OH-C=C-C=N- chromophore. When the concentration of Al^{3+} was gradually increased in the **SQ** system, the three main absorption peaks of **SQ** were gradually decreased, and new two enhanced absorption peaks were generated at 309 and 387 nm, which was attributed to the effective combination of **SQ** and Al^{3+}, equal absorption points were formed at 302 nm, 325 nm and 358 nm, which marked the equilibrium transition between free **SQ** and **SQ**-Al^{3+}. Similar to **SQ**, the free **NQ** had three main absorption peaks, the absorption peaks at 256 nm and 331 nm are due to the intramolecular n-π* electronic transition, and the 373 nm was due to the intramolecular π-π* electronic transition. After Al^{3+} gradually added to the **NQ** system, the most obvious was the new broadband absorption peak at 404-450 nm, and the absorption peak intensity at 373 nm gradually decreases, and the equal absorption points were formed at 349 nm and 395 nm, indicating the balance between **NQ** and **NQ**-Al^{3+}.

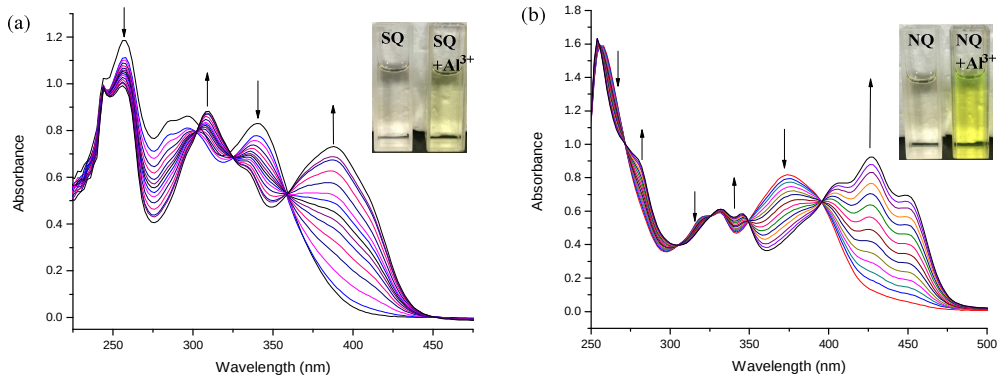

Fig. 4. (a) UV absorption spectrum changes of **SQ** (3.33×10^{-5} M) after adding different ratios of Al^{3+} in DMSO-H_2O (1/2, v/v) solution, inset: color change of **SQ** solution before and after adding Al^{3+} in day light; (b) The UV absorption spectrum of the solution changes after adding different ratios of Al^{3+} to **NQ** (3.33×10^{-5} M) DMSO-H_2O (1/2, v/v) solution, inset: color change of **NQ** solution before and after addition of Al^{3+} in day light.

3.3. Binding mode studies

In order to explore the complexation mode between **SQ** and **NQ** for Al^{3+}, the Job's curve was first plotted to estimate the stoichiometry of the complexation between the host and the metal ions, what should do was maintaining the total concentration of Al^{3+} and **SQ** or **NQ** at 1.00×10^{-4} M and changing the ratio (1:9-9:1) between Al^{3+} and **SQ** or **NQ**. The abscissa of largest fluorescence intensity gap was at 0.5, indicating that the ratio of **SQ** or **NQ** with Al^{3+} were both 1: 1 (Fig. s10), which was also supported by HRMS, Al^{3+} was added in **SQ** and **NQ** system and the peaks were captured at m/z 395.0579 and m/z 445.0732 respectively assigned to [**SQ**-Al^{3+}+NO_3^--H^+]$^+$ and [**NQ**-Al^{3+}+NO_3^--H^+]$^+$ (Fig. s11 and Fig. s12).

IR spectra was then made of **SQ**, **SQ**-Al^{3+} and **NQ**, **NQ**-Al^{3+} (Fig. s13), and 3452 and 3373 cm^{-1} were -OH stretching vibration belonging to the quinoline unit and salicylaldehyde unit in **SQ** and **NQ**, 3203 and 3226 cm^{-1} were stretching vibrations of amide NH, 3054 and 3060 cm^{-1} were due to the presence of quinoline ring, and 1622 and 1655 cm^{-1} were peaks of -C=O, and 1500 and 1502 cm^{-1} were attributed to the -C=N- extension vibration. When **SQ** combined with Al^{3+}, the phenolic hydroxyl stretching vibration at 3452 cm^{-1} disappeared and the peaks at 1622 and 1500 cm^{-1} also changed significantly, indicating that the phenolic hydroxyl atom, oxygen atom of the -C=O group and the nitrogen atom of the -C=N- group participated in the complexation with Al^{3+}. Similarly, when **NQ** complexes with Al^{3+},

the phenolic hydroxyl peak at 3373 cm^{-1} shifted to 3384 cm^{-1}, and the -C=N group at 1502 cm^{-1} disappeared, the stretching vibration peak at 1655 cm^{-1} was transferred to 1610 cm^{-1}, indicating that the oxygen atom of phenolic hydroxyl and -C=O group and the nitrogen atom of the imine group participated in complexation with Al^{3+}.

To further explore the complexation pattern of **SQ** or **NQ** with Al^{3+}, ^1H NMR titration experiment was performed in DMSO-d_6 solution. As shown in the Fig. 5, a, b, and c represented separately the NMR spectrum of only **SQ**, 0.5 equiv. Al^{3+}, 1.0 equiv. Al^{3+} to the **SQ** solution. With the gradual addition of Al^{3+}, the peak of the probe **SQ** changed significantly, and the proton signal peak (H1) of the phenolic hydroxyl group gradually disappeared, indicating that the O atom of phenolic hydroxyl participated in the coordination with Al^{3+}. The proton signal peak (H3) of the acidamide and the hydroxyl (H4) signal peak of the quinoline ring did not change significantly (the integral value did not change). The proton signal peak (H2) of the imine group (-CH=N-) shifted from 8.86 ppm to a high field to 8.84 ppm, indicating that the nitrogen atom of the imine group took part in the coordination with Al^{3+}. In addition, combining with HRMS data, we knew that Al^{3+} formed an additional coordinate bond with another oxygen atom through the nitrate anion. The same analyzed way was carried out for **NQ** and the results were given in the Fig. s14.

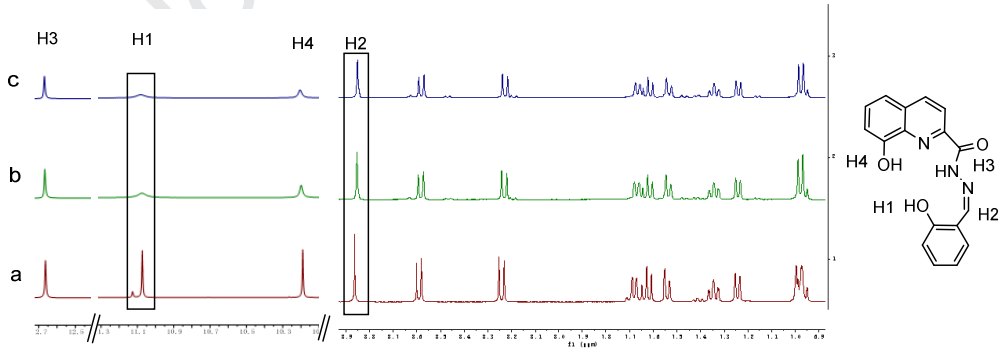

Fig. 5. ^1H NMR spectrum of (a) **SQ**, (b) 0.5 equiv. Al^{3+} and (c) 1.0 equiv. Al^{3+} added in DMSO-d_6.

In order to further explore the sensing mechanism between the probes **SQ** or **NQ** with Al^{3+}, we performed the B3LYP/6-31G(d) method on the Guassian 09 program for the optimization structures of the probe **SQ**, **NQ**, the complexes **SQ**-Al^{3+} and

NQ-Al^{3+} (Fig. 6 and Fig. 7). The quinolyl group and the phenol group of the free probe **SQ** were not in the same plane with the dihedral angle 35.46° formed, which was due to the isomerization of the -C=N- double bond in the **SQ** molecule. Upon complexation with Al^{3+}, the quinoline group and the phenol group formed a coplanarity with Al^{3+} such that inhibition of -C=N- double bond isomerization and attenuation of the non-radiative transition of the **SQ**, resulting in enhanced fluorescence. According to the results of NMR titration experiments and IR spectroscopy, it was found that Al^{3+} formed three coordination bonds with the carbonyl oxygen atom, nitrogen atom of the imine group and the oxygen atom of the phenolic hydroxyl group of **SQ**. The bond lengths of O-Al^{3+}, N-Al^{3+}, and O-Al^{3+} were 1.8372, 1.9681, and 1.7709 nm, respectively. In addition, Al^{3+} formed an additional coordinate bond with another oxygen atom through the nitrate anion. The HOMO and LUMO orbital energy gaps of **SQ** before and after complexing Al^{3+} were calculated by DFT. The energy gap difference between HOMO and LUMO of composite **SQ**-Al^{3+} (E=1.1070 eV) was much lower than that of **SQ** (E=3.8708 eV), which indicated that the free probe and Al^{3+} tend to complex and the thermodynamics of the complex **SQ**-Al^{3+} was stable. **NQ** was similar to the coordination of **SQ** and Al^{3+}. Combining with the above fluorescence and IR spectroscopy, HRMS and ^{1}H NMR titration, we proposed the possible complexation mode and sensing mechanism between the probes **SQ** or **NQ** with Al^{3+} and F^{-} (Scheme 2).

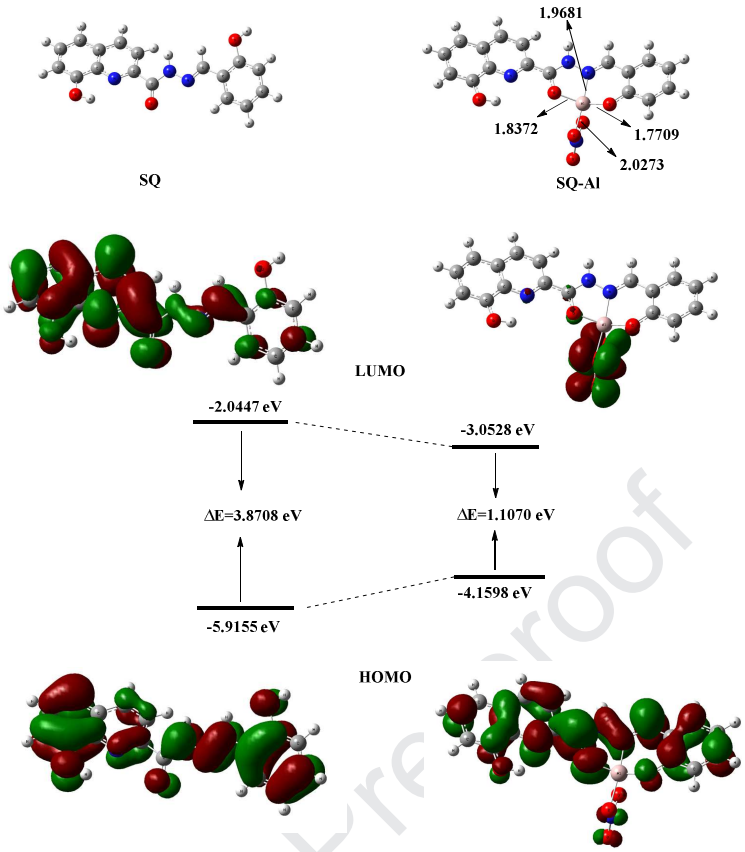

Fig. 6. Frontier molecular orbital of **SQ** and **SQ**-Al^{3+} complex.

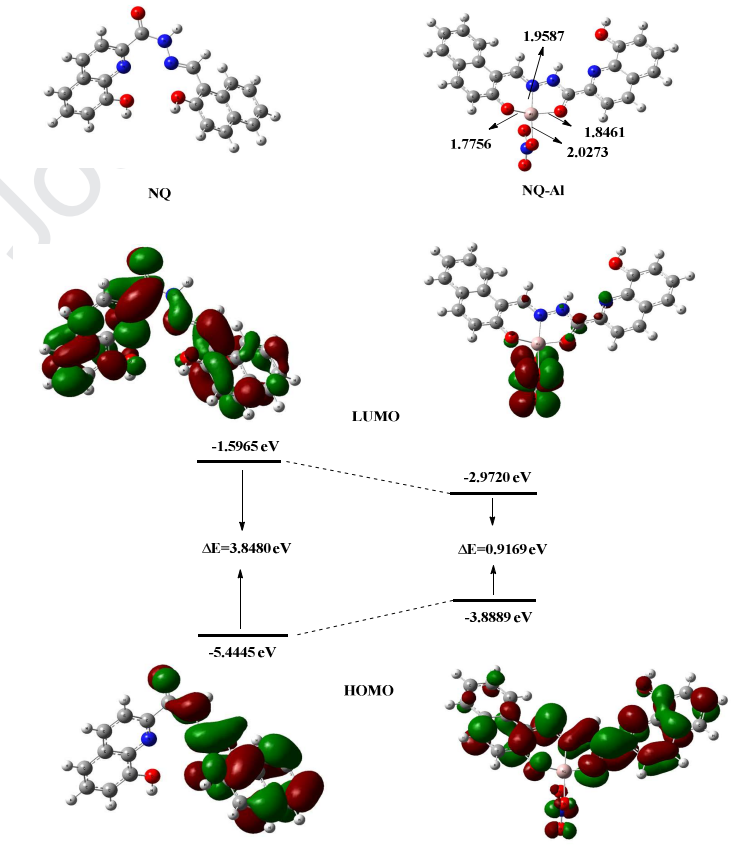

Fig. 7. Frontier molecular orbital of **NQ** and **NQ**-Al^{3+} complex.

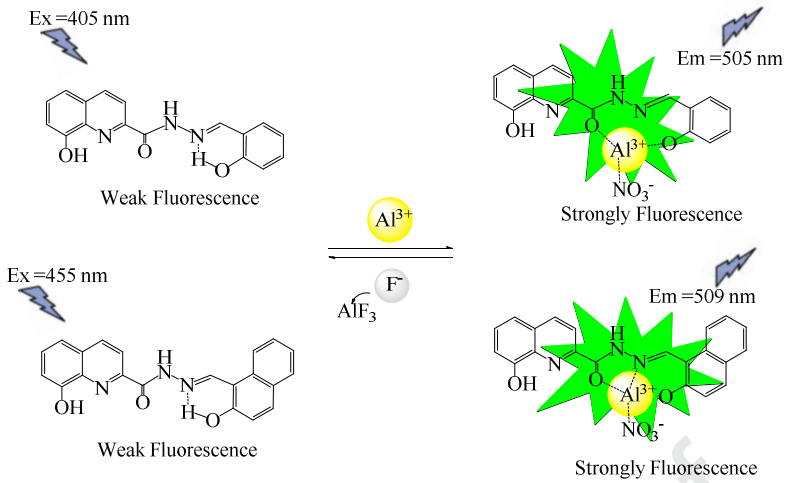

Scheme 2. The possible complexation mode and sensing mechanism between the probes **SQ** or **NQ** with Al^{3+} and F^{-}.

3.4. Determination of Al^{3+} in filter paper

In order to explore the field-test performance of probes **SQ** and **NQ**, a simple and direct filter paper experiment was conducted. In the first place, 3 μL solution of **SQ** (0.1 mM) in ethanol was prepared and dropped on the filter paper to give a dark yellow dot under the UV lamp. Furthermore, 1 μL metal ions (0.1 μM) to be tested were covered at the point of **SQ**. The test method of **NQ** was the same as **SQ**. The final consequence manifested that Al^{3+} presented a change in fluorescent color different from other metal ions (Fig. 8 and 9), which laid a foundation in practical applications.

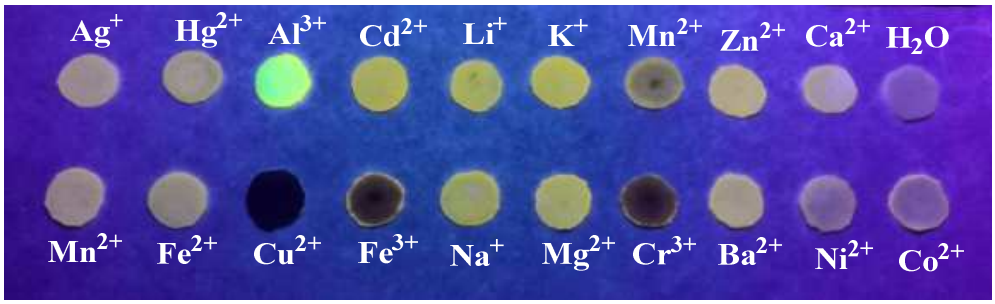

Fig. 8. Photographic image of metal ions by **SQ** on filter paper by UV-light (wavelength 365 nm).

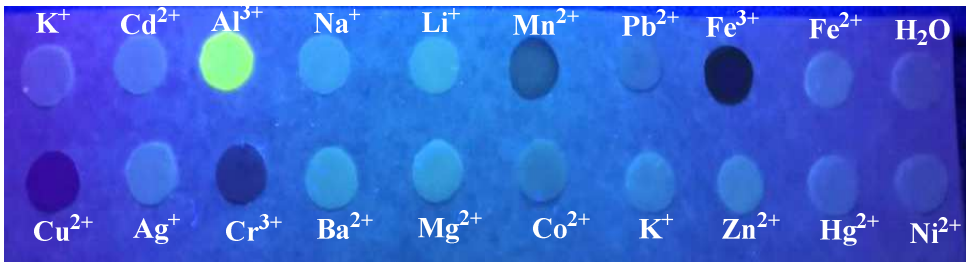

Fig. 9. Photographic image of metal ions by **NQ** on filter paper by UV-light (wavelength 365 nm).

*3.5. Spectroscopic studies of **SQ** and **NQ** on anions*

In view of the particular interaction, **SQ**-Al^{3+} and **NQ**-Al^{3+} were used as anion probes to perform anion screening, as shown in Fig. 10, different anions F^-, Cl^-, Br^-, I^-, PO_4^{3-}, SO_3^{2-}, NO_3^- , HSO_3^-, SCN^-, S^{2-}, CO_3^{2-}, HCO_3^-, $S_2O_8^{2-}$, HSO_4^-, $H_2PO_4^-$, $Cr_2O_7^{2-}$, SO_4^{2-}, HPO_4^{2-}, CH_3COO^-, PPi and citrate anion (0.1 M) were added respectively to **SQ**-Al^{3+} and **NQ**-Al^{3+} in DMSO-H_2O (1/2, v/v) solution to determine its selectivity for anion, and it was found that **SQ**-Al^{3+}, **NQ**-Al^{3+} produced fluorescence quenching effect only for F^- different from other anions, the resulting fluorescence intensity and color of solution were consistent with the initial free **SQ** and **NQ**.

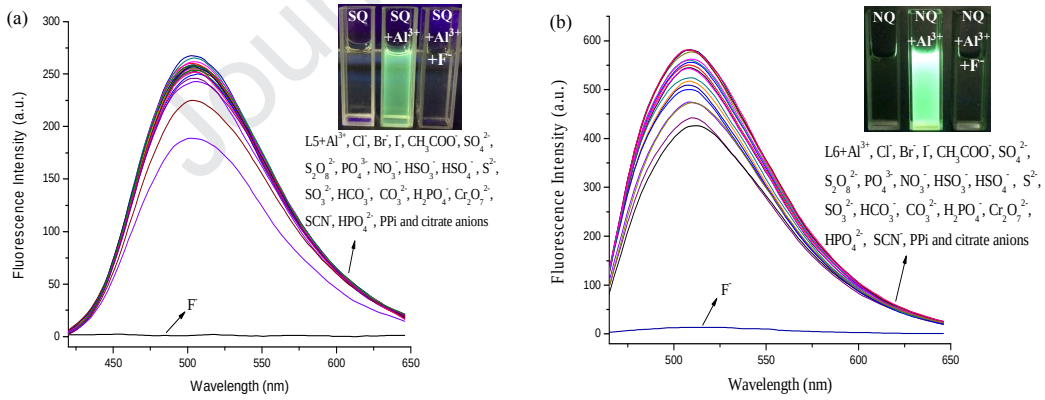

Fig. 10. (a) Fluorescence spectral changes of the **SQ**-Al^{3+} (3.33×10^{-5} M) solution after addition of different anions in DMSO-H_2O (1/2, v/v). Inset: color change of **SQ**-Al^{3+} before and after F^- added in; (b) Fluorescence spectral changes of the **NQ**-Al^{3+} (3.33×10^{-5} M) solution after addition of different anions in DMSO-H_2O (1/2, v/v). Inset: color change of the **NQ**-Al^{3+} solution before and after F^- added in.

A fluorescence competition experiment was then performed to detect the anti-interference recognition ability of **SQ** and **NQ** to identify F^- (Fig. s15). The above anions were added separately in the DMSO-H_2O (1/2, v/v) containing **SQ**-Al^{3+},

NQ-Al^{3+}, then F^- was added to these systems and fluorescence data were collected. The consequence suggested F^- still had obvious fluorescence quenching effect on **SQ**-Al^{3+} and **NQ**-Al^{3+}, which exhibited good anti-interference and selective recognition ability for F^-.

The fluorescence titration experiments were performed on **SQ**-Al^{3+} and **NQ**-Al^{3+} on F^- to explore their sensing properties (Fig. 11). Gradually increasing F^- in **SQ**-Al^{3+} and **NQ**-Al^{3+} (3.33×10^{-5} M) solutions respectively and collecting fluorescence data. It was found that the fluorescence emission peaks of **SQ**-Al^{3+} at 505 nm and **NQ**-Al^{3+} at 509 nm became reduced, until the F^- concentration reaching at 1.88 and 1.68 equiv., the fluorescence intensity got equilibrium, which was due to the F^- gradual pulled Al^{3+} out from the **SQ**-Al^{3+} and **NQ**-Al^{3+} complexes and released free **SQ** and **NQ**. This result was proved in HRMS, after adding F^- in the systems of **SQ**-Al^{3+} and **NQ**-Al^{3+}, respectively, the peaks of **SQ** and **NQ** were captured at m/z 308.1033 and m/z 358.1190, which were assigned as [**SQ**+H^+] and [**NQ**+H^+] (Fig. s16 and Fig. s17). The detection limits of **SQ**-Al^{3+} and **NQ**-Al^{3+} for F^- were calculated to be 1.64×10^{-7} and 3.58×10^{-8} M, respectively (Fig. s18).

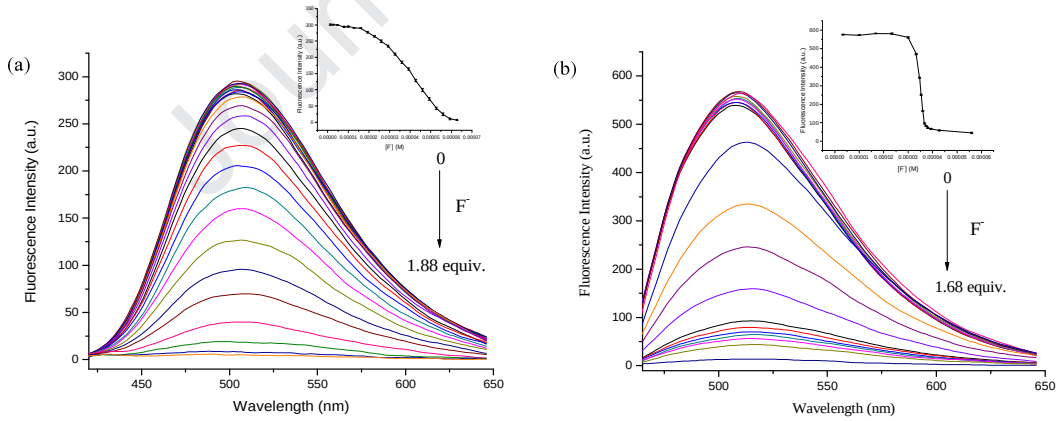

Fig. 11. (a) Fluorescence titration of **SQ**-Al^{3+} (3.33×10^{-5} M) in the DMSO-H_2O (1/2, v/v) solution with different concentration of F^- (0-1.88 equiv.) added; (b) Fluorescence titration of **NQ**-Al^{3+} (3.33×10^{-5} M) in the DMSO-H_2O (1/2, v/v) solution with different concentration of F^- (0-1.68 equiv.) added. Inset: error bars were obtained from the standard deviation of three replicate experiments.

In the UV-visible titration experiment of **SQ**-Al^{3+} and **NQ**-Al^{3+} on F^- (Fig. 12), it was found that the main absorption peaks of **SQ**-Al^{3+} at 309 and 387 nm gradually

decreased while the F^- concentration increasing in the system, and the absorption peaks at 257 and 340 nm increased. The absorption peak intensity at 405-450 nm of **NQ**-Al^{3+} gradually decreased while the peak at 373 nm gradually increased, and the peak between 250-349 nm gradually recovered to the same as free **NQ**, which indirectly proved that the presence of F^- was to pull Al^{3+} out in the **SQ**-Al^{3+} and **NQ**-Al^{3+} systems, releasing free **SQ** and **NQ**.

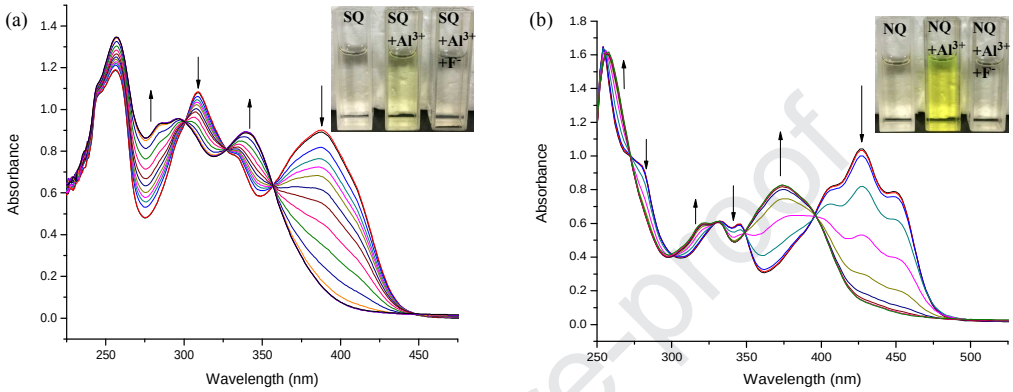

Fig. 12. (a) UV absorption spectrum changes of addition different ratios of F^- to **SQ**-Al^{3+} (3.33×10^{-5} M) DMSO-H_2O (1/2, v/v) solution, inset: color change of **SQ**-Al^{3+} solution before and after F^- addition; (b) UV absorption spectrum changes of addition different ratios of F^- to **SQ**-Al^{3+} (3.33×10^{-5} M) DMSO-H_2O (1/2, v/v) solution, inset: color change of **NQ**-Al^{3+} solution before and after F^- addition.

Next, the reversibility of probes **SQ** and **NQ** was explored to identify Al^{3+} and F^- (Fig. s19). Al^{3+} and F^- were alternately added to the **SQ** and **NQ** solutions which caused switchable fluorescence changes and this reversible cycle can be repeated several times, indicating that **SQ** and **NQ** can have an "on" fluorescence response to Al^{3+}, while the **SQ**-Al^{3+} and **NQ**-Al^{3+} complexes exhibited a "off" fluorescence response to F^-. After several repetitions, the recognition efficiency of the probes **SQ** and **NQ** for Al^{3+} and F^- was still appreciable.

*3.6. pH affection to the recognition of **SQ** and **NQ***

pH tests was performed on **SQ** and **NQ** in DMSO-H_2O (1/2, v/v) systems (Fig. s20) to explore their effect on recognition for Al^{3+} and F^-. The fluorescence emission states of **SQ** and **NQ** were relatively stable at the physiological pH (6.3~9.3 and 6.3~10.3), but the recognition abilities of **SQ** and **NQ** for Al^{3+} were affected in both high acid (pH < 5.3) and high alkali (pH > 10.3). The recognition effect of **SQ**-Al^{3+}

and **NQ**-Al^{3+} on F^- was relatively stable. This phenomenon in vitro at physiological pH laid a favorable foundation for us to carry out in-vivo object recognition, and it is expected to be applied in food, environment and organisms.

3.7. MTT assay and Cell imaging

To explore the prospect of application value of probes **SQ** or **NQ** in organisms, MTT assay in PC12 cells was preferentially executed to assess the toxicity of **SQ** and **NQ** to cells at different concentrations 0, 30, 60, 90, 120 μM and the consequence indicated that **SQ** was amicable on cells viability even at high concentration, but **NQ**, to a certain extent, may exist some threat at high concentration. The fluorescence imaging experiment was next performed in biological cells. PC12 cells were firstly incubated with 20 μM **SQ** and **NQ** in sterile PBS at 37 °C for 30 min, then were washed three times with PBS buffer and observed under a fluorescent inverted microscope. The bright field image indicated good cell configuration (Fig. 13a and 13g), which did not appear fluorescence in dark field (Fig. 13b and 13h). Then, the cells culture medium with **SQ** and **NQ** was incubated with 30 μM Al^{3+} for 20 min. After the incubation, the cells were washed three times with PBS buffer, and observed. The cells showed brightness and green fluorescence under dark field (Fig. 13d and 13j). Finally, when we continued to add 40 μM F^- into the cells for another 20 min, the fluorescence of the cells in the dark field was quenched (Fig. 13f and 13l), which was consistent with the analysis obtained in our fluorescence spectra.

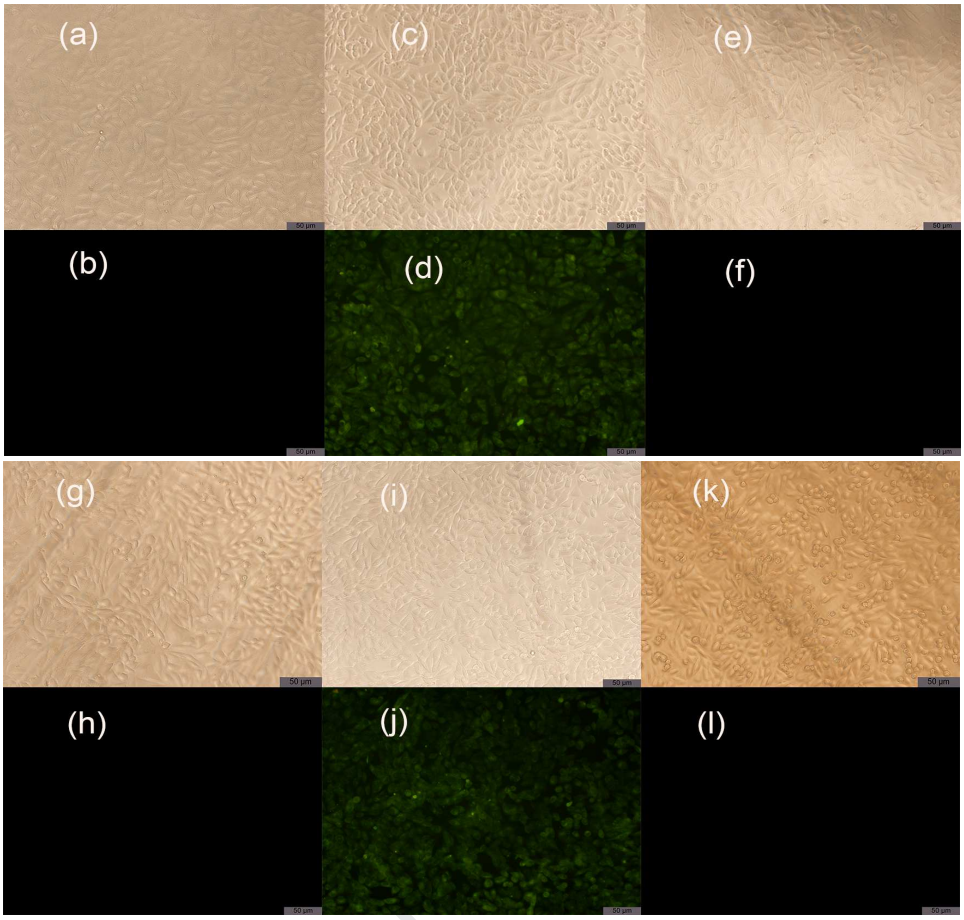

Fig. 13. (a) Bright-field fluorescence microscopic image of live PC12 cells only cultured with **SQ**; (b) Dark-field fluorescence microscopic image of a; (c) Bright-field fluorescence microscopic image treated with Al^{3+} after a; (d) Dark-field fluorescence microscopic image of c; (e) Bright-field fluorescence microscopic with F^- treated after c; (f) Dark-field fluorescence microscopic image of e; (g) Bright-field fluorescence microscopic image of live PC12 cells only cultured with **NQ**; (h) Dark-field fluorescence microscopic image of g; (i) Bright-field fluorescence microscopic image with Al^{3+} treated after g; (j) Dark-field fluorescence microscopic image of i; (k) Bright-field fluorescence microscopic image with F^- treated after i; (l) Dark-field fluorescence microscopic image of k. Scale bars: 50 μm.

4. Conclusion

In summary, the probes **SQ** and **NQ** based on 8-hydroxyquinoline revealed sequentially recognition towards Al^{3+} and F^- (λ_{ex}: 405 and 455 nm) with obvious vision changes of color as well as an 'OFF-ON-OFF' fluorescent response in DMSO-H_2O (1/2, v/v) solution. The detection limits of **SQ** and **NQ** for Al^{3+} were 1.48×10^{-8} and 4.23×10^{-8} M and for F^- 1.64×10^{-7} and 3.58×10^{-8} M, respectively. The complexation mode between the probes **SQ** or **NQ** and Al^{3+} was inferred by fluorescence spectra, UV spectra, HRMS and NMR titration to obtain a 1:1 complex, which was through ESIPT and CHEF mechanism. DFT calculation also simulated the

distribution of electron clouds and energy changes before and after mating. In addition, filter paper and cell imaging experiments proved the probes **SQ** and **NQ** had the potential application value to monitor Al^{3+} and F^- in environment and vivo.

Acknowledgements

We thank the Natural Science Foundation of China (No. U1404207) for financial support.

References

[1] M. Iniya, D. Jeyanthi, K. Krishnaveni, A. Mahesh, D. Chellappa, Triazole based ratiometric fluorescent probe for Zn^{2+} and its application in bioimaging, Spectrochim. Acta A 120 (2014) 40–46.

[2] J. X. Fu, Y. X. Chang, B. Li, H. H. Mei, L. Yang, K. X. Xu, A novel fluorescent-colorimetric probe for Al^{3+} and Zn^{2+} ion detection with different response and applications in F^- detection and cell imaging, Analyst, 144 (2019) 5706–5716.

[3] N. Gupta, S. S. Gaurav, A. Kumar, Molecular basis of aluminium toxicity in plants: a review, Am. J. Plant Sci. 4 (2013) 21–37.

[4] J. R. Walton, Aluminum in hippocampal neurons from humans with Alzheimer's disease, Neurotoxicology 27 (2006) 385–394.

[5] E. Altschuler, Aluminum-containing antacids as a cause of idiopathic Parkinson's disease, Med. Hypotheses 53 (1999) 22–23.

[6] G. Muller, V. Bernuzzi, D. Desor, M. F. Hutin, D. Burnel, P. R. Lehr, Developmental alterations in offspring of female rats orally intoxicated by aluminum lactate at different gestation periods, Teratology 42 (1990) 253–261.

[7] X. H. Luo, X. Y. Li, Y. Wang, X. M. Xie, L. Yang, A Novel Reversible Fluorescent Probe for Sequential Detection of Aluminium Ion and PPi and Bioimaging in Living Cells, Chemistryselect 4 (2019) 10643–10648.

[8] M. A. Qadir, M. Ahmed, S. Shahzad, Determination of Aluminium by electrothermal atomization atomic absorption spectrometry in serum to characterize hemodialysis toxicity, Anal. Lett. 48 (2015) 147–153.

[9] S. Noremberg, M. Veiga, D. Bohrer, C. Viana, P. C. do Nascimento, L. M. de

Carvalho, P. Mattiazzi, Determination of aluminum and silicon in bovine liver by graphite furnace atomic absorption spectrometry after dissolution with tetramethylammonium hydroxide, Anal. Method 7 (2015) 500–506.

[10] B. Peng, D. Wu, J. Lai, H. Xiao, P. Li, Simultaneous determination of halogens (F, Cl, Br, and I) in coal using pyrohydrolysis combined with ion chromatography, Fuel 94 (2012) 629–631.

[11] A. Pandey, A. Kelkar, R. K. Singhal, C. Baghra, A. Prakash, M. Afzal, J. P. Panakkal, Effect of accelerators on thoria based nuclear fuels for rapid and quantitative pyrohydrolytic extraction of F^- and Cl^- and their simultaneous determination by ion chromatography, J. Radioanal. Nucl. Chem. 293 (2012) 743–749.

[12] A. Martin-Camean, A. Jos, M. Puerto, A. Calleja, A. Iglesias-Linares, E. Solano, A. M.Cameán, In vivo determination of aluminum, cobalt, chromium, copper, nickel, titanium and vanadium in oral mucosa cells from orthodontic patients with mini-implants by Inductively coupled plasma-mass spectrometry (ICP–MS), J. Trace Elem. Med. Biol. 32 (2015) 13–20.

[13] A. Saha, D. Shah, S. B. Deb, M. K. Saxena, V. G. Mishra, B. K. Nagar, B. S.Tomar, Simultaneous quantification and isotope ratio measurement of boron in uranium-silicon-aluminium compounds by inductively coupled plasma orthogonal acceleration time of flight mass spectrometry (ICP–OA–TOFMS) after its separation by pyrohydrolysis, Microchem. J. 121 (2015) 56–64.

[14] J. Wang, W. Lin, W. Li, Single fluorescent probe displays a distinct response to Zn^{2+} and Cd^{2+}, Chem. Eur. J. 18 (2012) 13629–13632.

[15] J. Y. Zhang, B. L. Xing, J. Z. Song, F. Zhang, C. Y. Nie, L. Jiao, L. B. Liu, F. T. Lv, S. Wang, Associated analysis of DNA methylation for cancer detection using CCP-Based FRET technique, Anal. Chem. 86 (2014) 346–350.

[16] Y. X. Chang, B. Li, Y. F. Gao, K. X. Xu, A novel Schiff-base fluorescent probe for Cr^{3+} and its bioimaging in cells, Chin. J. Org. Chem. 39 (2019) 1023–1028.

[17] A. T. Wright, E.V. Anslyn, Differential receptor arrays and assays for solution-based molecular recognition, Chem. Soc. Rev. 35 (2006) 14–28.

[18] V. Amendola, L. Fabbrizzi, Anion receptors that contain metals as structural units, Chem. Commun. 5 (2009) 513–531.

[19] L. Prodi, Luminescent chemosensors: from molecules to nanoparticles, New J.

Chem. 29 (2005) 20–31.

[20] J. Xu, S. Sun, Q. Li, Y. Yue, Y. Li, S. Shao, A novel Turn-On fluorescent probe for F^- detection in aqueous solution and its application in live-cell imaging, Anal. Chim. Acta 849 (2014) 36–42.

[21] K. Yao, Y. X. Chang, B. Li, H. Yang, K. X. Xu, A novel coumarin-based fluorescent sensor for Ca^{2+} and sequential detection of F^- and its live cell imaging, Spectrochim. Acta A 216 (2019) 385–394.

[22] R. P. Schwarzenbach, B. I. Escher, K. Fenner, T. B. Hofstetter, C. A. Johnson, U. von Gunten, B. Wehrli, The challenge of micropollutants inaquatic systems, Science 313 (2006) 1072–1077.

[23] S. Jagtap, M. K. Yenkie, N. Labhsetwar, S. Rayalu, Fluoride in drinking water and defluoridation of water, Chem. Rev. 112 (2012) 2454–2466.

[24] X. C. Fu, J. Z. Jin, J. Wu, J. C. Jin, C. G. Xie, A novel turn-on fluorescent sensor for highly selective detection of Al(III) in an aqueous solution based on simple electrochemically synthesized carbon dots, Anal. Methods 9 (2017) 3941–3948.

[25] L. Fan, J. Qin, T. Li, B. Wang, Z. Yang, A novel rhodamine chromone-based "Off–On" chemosensor for the differential detection of Al(III) and Zn(II) in aqueous solutions, Sens. Actuators B 203 (2014) 550–556.

[26] S. K. Shoora, A. K. Jain, V. K. Gupta, A simple Schiff base based novel optical probe for aluminium (III) ions, Sens. Actuators B 216 (2015) 86–104.

[27] M. Mukherjee, S. Pal, S. Lohar, B. Sen, S. Banerjee, S. Banerjee, P. Chattopadhyay, A napthelene–pyrazol conjugate: Al(III) ion-selective blue shifting chemosensor applicable as biomarker in aqueous solution, Analyst 139 (2014) 4828–4835.

[28] J. M. Lehn, Sopramplecular chemistry, Science 260 (1993) 1762–1763.

[29] J. M. Lehn, Supramolecular chemistry-concepts and perspectives, WileyVCH, 1995.

[30] J. Xue, L. M. Tian, Z. Y. Yang, A novel ratiometric fluorescent probe based on coumarin derivative for the recognition of Al(III) and its application on test strips, Tetrahedron Lett. 60 (2019) 150945-150950.

[31] L. Fan, J. C. Qin, C. R. Li, Z. Y. Yang, A Schiff-base receptor based chromone derivate: Highly selective fluorescent and colorimetric probe for Al(III),

Spectrochim. Acta A 218 (2019) 342–347.

[32] B. J. Pang, C. R. Li, Z. Y. Yang, Design of a colorimetric and turn-on fluorescent probe for the detection of Al(III), Journal of Photoch. Photobio. A 356 (2018) 159–165.

[33] T. Anand, G. Sivaraman, A. Mahesh, D. Chellappa, Aminoquinoline based highly sensitive fluorescent sensor for lead(II) and aluminum(III) and its application in live cell imaging, Anal. Chim. Acta 853 (2015) 596–601.

[34] H. Y. Liu, B. B. Zhang, C.Y. Tan, F. Liu, J. K. Cao, Y. Tan, Y. Y. Jiang, Simultaneous bioimaging recognition of Al^{3+} and Cu^{2+} in living-cell, and further detection of F^{-} and S^{2-} by a simple fluorogenic benzimidazole-based chemosensor, Talanta 161 (2016) 309–319.

[35] Y. W. Choi, G. J. Park, Y. J. Na, H.Y. Jo, S. A. Lee, G. R. You, C. Kim, A single schiff base molecule for recognizing multiple metal ions: A fluorescence sensor for Zn(II) and Al(III) and colorimetric sensor for Fe(II) and Fe(III), Sens. Actuators B 194 (2014) 343–352.

[36] Q. P. Diao, P. Y. Ma, L. L. Lv, T. C. Li, Y. Sun, X. H. Wang, D. Q. Song, A water-soluble and reversible fluorescent probe for Al^{3+} and F^{-} in living cells, Sens. Actuators B 229 (2016) 138–144.

[37] V. S. Gopinath, J. Pinjari, R. T. Dere, Design, synthesis and biological evaluation of 2-substituted quinolines as potential antileishmanial agents, Eur. J. Med. Chem, 69 (2013) 527-536.

[38] P. Wang, J. X. Fu, K. Yao, Y. X. Chang, K. X. Xu, Y. Q. Xu, A novel quinoline-derived fluorescent “turn-on” probe for Cu^{2+} with highly selectivity and sensitivity and its application in cell imaging, Sens. Actuators B 273 (2018) 1070–1076.

[39] G. Q. Yang, F. Morlet-Savary, Z. K. Peng, S. K. Wu, J. P. Fouassier, Triplet-triplet absorption of 2-(2′-hydroxyphenyl) benzoxazole (HBO) in polar solvents, Chem. Phys. Lett. 256 (1996) 536–542.

[40] J. X. Fu, K. Yao, Y. X. Chang, B. Li, L. Yang, K. X. Xu, A novel colorimetric-fluorescent probe for Al^{3+} and the resultant complex for F^{-} and its

applications in cell imaging, Spectrochim. Acta A 222 (2019) 117234–117245.

[41] M. Royzen, A. Durandin, V. G. Young, N. E. Geacintov, J. W. Canary, A sensitive probe for the fetection of Zn(II) by time-resolved fluorescence, J. Am Chem. Soc. 128 (2006) 3854–3855.

[42] K. Yao, J. X. Fu, Y. X. Chang, B. Li, L. Yang, K. X. Xu, A selective fluorescent probe for relay detection of Zn^{2+} and tartrate: Application to logic circuit and living cell imaging, Spectrochim. Acta A 205 (2018) 410–418.

[43] L. N. Wang, W. W. Qin, X. L. Tang, W. Dou. Development and applications of fluorescent indicators for Mg^{2+} and Zn^{2+}, J. Phys. Chem. A 115 (2011) 1609–1616.

[44] C. B. Murray, D. J. Noms, M. G. Bawendi, Synthesis and characterization of nearly monodisperse CdE (E = sulfur, selenium, tellurium) semiconductor nanocrystallites, J. Am. Chem. Soc. 115 (1993) 8706–8715.

[45] X. Y. Liu, P. Wang, J. X. Fu, K. Yao, K. Xue, K. X. Xu, Turn-on fluorescent sensor for zinc and cadmium ions based on quinolone and its sequential response to phosphate, J. Lumin. 186 (2017) 16–22.

[46] C. Y. Wang, J. X. Fu, K. Yao, Y. X. Chang, L. Yang, K. X. Xu, Development of acridine-derived “turn on” Al^{3+} fluorescent sensors and their imaging in living cells, Chemistry Select 3 (2018) 2805–2811.

[47] C. Kim, S. Hwang, M. Kin, M. Lee, M. H. Lim, A single fluorescent chemosensor for multiple targets: the sequential detection of Al^{3+} and pyrophosphate and the selective detection of F^{-} in a near-perfect aqueous solution, New J. Chem. 41 (2017) 15590–15600.

1. Two fluorescent 8-hydroxyquinoline-based probes **SQ** and **NQ** were synthesized.
2. The probes **SQ** and **NQ** for the sequentially detected of Al^{3+} and F^{-} in aqueous solutions.
3. The binding modes of probes **SQ** and **NQ** with $Al^{3+}$and F^{-} had been well demonstrated by ESI-MS, ^{1}H NMR and DFT calculation.
4. The filter paper and cell imaging experiments proved probes **SQ** and **NQ** had the potential application value to monitor Al^{3+} and F^{-} in environment and vivo.

Declaration of interests

The authors declare that they have no known competing financial interests or personal relationships that could have appeared to influence the work reported in this paper.